

OPEN

Nitro-fatty acids suppress ischemic ventricular arrhythmias by preserving calcium homeostasis

Martin Mollenhauer^{1,2,12}✉, Dennis Mehrkens^{1,2,12}, Anna Klinke³, Max Lange^{1,2}, Lisa Remane^{1,2}, Kai Friedrichs³, Simon Braumann^{1,2}, Simon Geißen^{1,2}, Sakine Simseyilmaz^{1,2}, Felix S. Nettersheim^{1,2}, Samuel Lee^{1,2}, Gabriel Peinkofer^{1,2}, Anne C. Geisler⁴, Bianca Geis⁴, Alexander P. Schwoerer⁵, Lucie Carrier⁶, Bruce A. Freeman⁷, Matthias Dewenter^{8,9}, Xiaojing Luo¹⁰, Ali El-Armouche¹⁰, Michael Wagner^{10,11}, Matti Adam^{1,2}, Stephan Baldus^{1,2} & Volker Rudolph³

Nitro-fatty acids are electrophilic anti-inflammatory mediators which are generated during myocardial ischemic injury. Whether these species exert anti-arrhythmic effects in the acute phase of myocardial ischemia has not been investigated so far. Herein, we demonstrate that pretreatment of mice with 9- and 10-nitro-octadec-9-enoic acid (nitro-oleic acid, NO₂-OA) significantly reduced the susceptibility to develop acute ventricular tachycardia (VT). Accordingly, epicardial mapping revealed a markedly enhanced homogeneity in ventricular conduction. NO₂-OA treatment of isolated cardiomyocytes lowered the number of spontaneous contractions upon adrenergic isoproterenol stimulation and nearly abolished ryanodine receptor type 2 (RyR2)-dependent sarcoplasmic Ca²⁺ leak. NO₂-OA also significantly reduced RyR2-phosphorylation by inhibition of increased CaMKII activity. Thus, NO₂-OA might be a novel pharmacological option for the prevention of VT development.

Due to significant advances in the therapy of acute myocardial ischemia (AMI), e.g. more aggressive approaches to coronary revascularization and secondary prevention, AMI mortality has declined drastically over the last decades¹. However, patients suffering from AMI with ventricular tachycardia (VT) or -fibrillation (VF), still have a fourfold increased risk of in-hospital mortality².

The mechanisms accounting for the development of acute VT are diverse: in the acute ischemic phase, 15–30 min after AMI, the development of so called 1B arrhythmias has been linked to increased catecholamine release and disturbances in Ca²⁺ signaling within cardiomyocytes of the ischemic border zone, thus leading to ventricular conduction blocks and enhanced VT vulnerability^{3,4}. In particular, oxidation and subsequent autophosphorylation of Ca²⁺/calmodulin dependent kinase II (CaMKII) cause malfunctioning of ryanodine receptor type 2 (RyR2) channels and dysregulation of phospholamban (PLN)-dependent cytosolic Ca²⁺ clearance leading to an intracellular Ca²⁺ leak from the sarcoplasmic reticulum (SR)^{5,6}. Consequently, depolarization

¹Clinic III for Internal Medicine, Department of Cardiology, Center for Molecular Medicine Cologne (CMC), University of Cologne, Kerpener Str. 62, 50937 Cologne, Germany. ²Center for Molecular Medicine Cologne, CMC, University of Cologne, Cologne, Germany. ³Clinic for General and Interventional Cardiology/ Angiology, Herz- Und Diabeteszentrum NRW, Ruhr-Universitaet Bochum, Bad Oeynhausen, Germany. ⁴General and Interventional Cardiology University Heart Center Hamburg, University Hospital Hamburg-Eppendorf (UKE), Hamburg, Germany. ⁵Department of Cellular and Integrative Physiology, University Medical Center Hamburg Eppendorf, DZHK (German Centre of Cardiovascular Research), Partner Site Hamburg/Kiel/Lübeck, Hamburg, Germany. ⁶Experimental Pharmacology and Toxicology, University Hospital Hamburg-Eppendorf (UKE), Hamburg, Germany. ⁷Department of Pharmacology and Chemical Biology, University of Pittsburgh, Pittsburgh, PA, USA. ⁸Institute of Experimental Cardiology, University of Heidelberg, Heidelberg, Germany. ⁹German Centre for Cardiovascular Research (DZHK), Partner Site, Heidelberg/Mannheim, Germany. ¹⁰Department of Pharmacology and Toxicology, Technische Universitaet Dresden, Dresden, Germany. ¹¹Clinic for Internal Medicine and Cardiology, Heart Center Dresden, Dresden, Germany. ¹²These authors contributed equally: Martin Mollenhauer and Dennis Mehrkens. ✉email: martin.mollenhauer@uk-koeln.de

of the membrane potential is enhanced thereby causing inactivation of Na⁺ channels with further slowing of ventricular conduction⁷.

As the identification of AMI patients at risk for VT remains difficult, a therapeutic strategy would have to be applied to a broad patient population. Therefore, dietary intervention with endogenously produced anti-arrhythmic modulators appears as an attractive therapeutic approach. This concept has been recently supported by the randomized double blind trial *REDUCE-IT* which demonstrates that prophylactic treatment with icosapentaenoic acid-ethyl (VASCEPA) significantly reduces cardiovascular events, the rate of cardiac arrests, and the number of sudden cardiac deaths (SCD)⁸.

Nitro-oleic acid (9- and 10-nitro-octadec-9-cis-enoic acid; NO₂-OA) is an endogenously generated unsaturated fatty acid nitroalkene derivative that is formed by oleic acid reaction with nitric oxide and nitrite-derived nitrogen dioxide (•NO₂)^{9,10}. NO₂-OA is conferred with an electrophilic β-carbon that rapidly and reversibly reacts with nucleophilic cysteine-, and to a lesser extent histidine, residues via a Michael addition¹¹. The covalent nitro adduct is essential for the metabolic effects of NO₂-OA since native oleic acid is not electrophilic and ineffective in various studies^{12–14}. Nitro-fatty acids have been identified as potent endogenous anti-inflammatory mediators that affect a number of signaling mediators, transcriptional regulatory proteins and ion channels, including nuclear factor 'kappa-light-chain-enhancer' of activated B-cells (NF-κB), kelch-like ECH-associated protein 1 (Keap1/Nrf2), mitogen-activated protein kinases (MAPK), peroxisome proliferator-activated receptor gamma (PPARγ) and transient receptor potential channels (TRP) channels^{15–17}. Preclinical studies have demonstrated therapeutic benefit in a variety of disease models such as pulmonary hypertension, nephritis and, of relevance to herein, reperfusion damage after myocardial ischemia (I/R) and a subsequent attenuation of cardiac fibrosis, reduced infarct size and preserved left ventricular function^{18–20}. Since NO₂-OA has passed safety clinical phase I trials²¹ these results have been translated into two, currently recruiting, clinical phase II trials targeting pulmonary hypertension and primary focal segmental glomerular sclerosis^{22,23}.

Very low levels of NO₂-OA could be detected in human serum- and urine²⁴ as well as in the myocardium of rodents¹⁹. Nonetheless, inflammatory stimuli like I/R induce substantial generation of NO₂-OA up to μM concentrations by enhanced formation of nitrating species¹⁹. Furthermore, increased endogenous formation of nitro-linoleic acid has been demonstrated in healthy humans after dietary supplementation with conjugated linoleic acid and nitrite or nitrate²⁵.

If anti-arrhythmic effects of nitro-fatty acids could indeed be shown, a dietary supplementation or a pure pharmaceutical-based nitro-fatty acid therapeutic strategy in patients at risk for cardiovascular events could evolve as a strategy for prevention of sudden cardiac death.

Results

Susceptibility to VT upon right ventricular stimulation. Susceptibility to VT induction 20 min after ligation of the left anterior descending artery (LAD) was drastically reduced in animals pretreated with NO₂-OA (representative ECG recordings shown in Fig. 1A). Thus, the probability of VT induction, calculated as the percentage of induced VT episodes per stimulation maneuvers (Fig. 1B), as well as the total number of inducible VT episodes (Fig. 1C) were both significantly lower in NO₂-OA pretreated animals. Additionally, the total time of VT episodes was reduced after NO₂-OA-pretreatment (Fig. 1D) indicating that VT episodes in NO₂-OA pretreated ischemic hearts were rapidly self-terminating.

Homogeneity of conduction. Epicardial mapping studies within the peri-ischemic region (positioning of the multi-electrode array (MEA) is shown in Fig. 2A) clearly revealed a more homogeneous conduction pattern in NO₂-OA pretreated- compared to vehicle treated animals (representative conduction maps are shown in Fig. 2B). Of interest, only weak and therefore unevaluable electrical signals were detectable within the core ischemic region (data not shown). The mean electrical latency, measured apico-septally next to the ischemic core region²⁶, was significantly elevated after ischemia induction, indicating a reduction of electrical conduction velocity. Although latency was numerically lower in NO₂-OA pretreated hearts as compared to controls, it failed to reach statistical significance (Fig. 2C). However, the index of inhomogeneity was significantly lower upon administration of NO₂-OA, indicating a reduction in ventricular conduction blocks (Fig. 2D)²⁷.

To investigate potential side effects of NO₂-OA on action potential (AP) development, we performed patch-clamp analysis of isolated adult cardiomyocytes under baseline conditions. The treatment with NO₂-OA revealed no differences in the AP morphology regarding resting potential (Supplemental Fig. 1A), AP overshoot, (Supplemental Fig. 1B) or AP duration (APD, Supplemental Fig. 1C) between control and NO₂-OA treated cells.

Ca²⁺ transient analyses under isoproterenol treatment. Given that catecholamine induced disturbances in Ca²⁺ homeostasis are a major contributor to arrhythmia development in acute ischemia³, we investigated cytosolic Ca²⁺ transients and arrhythmic events in isolated adult cardiomyocytes by ratiometric fluorescence imaging (IonOptix Corp)²⁸. The number of arrhythmic events which appeared aside from a basic 1 Hz pacing stimulus (e.g. caused by early after depolarizations (EAD) and delayed after depolarizations (DAD)), was increased after beta-adrenergic stimulation with isoproterenol (Iso)³. Crucially, this increase was prevented by NO₂-OA treatment (Fig. 3A). Further investigation of single cellular calcium transients revealed that the time to Ca²⁺ peak concentration upon Iso challenge (Fig. 3B) was reduced after NO₂-OA treatment indicating a faster cytosolic Ca²⁺ influx. Furthermore, an increased peak height of the Ca²⁺ transient (Fig. 3C) was noted in both Iso treated groups as compared to vehicle treatment indicating elevated cytosolic Ca²⁺ levels. Accordingly, adrenergic stimulation led to a faster cytosolic Ca²⁺ clearance, as indicated by the reduced time to reach 50% or 90% of the maximum cellular Ca²⁺ concentration relative to baseline levels (Fig. 3D, E). Of note, no differences by additional NO₂-OA treatment were detected.

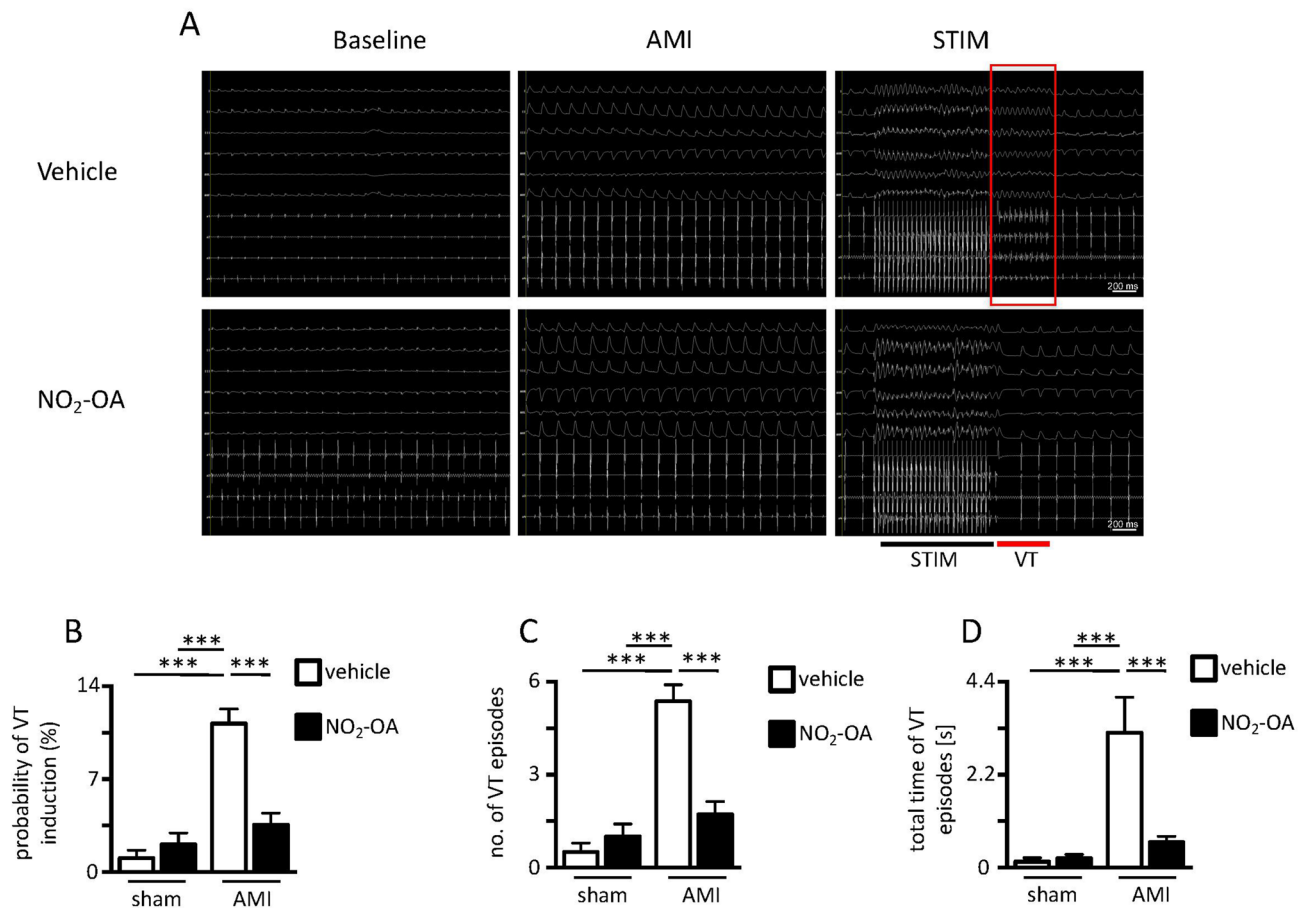


Figure 1. Surface and intracardiac electrocardiograms (ECG) of NO₂-OA versus vehicle treated mice. (A) Representative images of ECG before induction of myocardial ischemia (Baseline; left panel), 20 min after ischemia induction without right ventricular stimulation (AMI; middle panel) and after right ventricular stimulation (STIM; right panel) with appearance of ventricular tachycardias (VT) in NO₂-OA- or vehicle treated mice. Scale bar = 200 ms. (B) Probability of VT in sham versus LAD-ligated mice (AMI) with and without NO₂-OA treatment (AMI vehicle: 11.2 ± 3.1% vs. AMI NO₂-OA: 3.6 ± 2.3; n = 8/7). (C) Number of VT episodes (AMI vehicle: 5.4 ± 1.5 vs. AMI NO₂-OA: 1.7 ± 1.1; n = 8/7) and (D) Total time of VT episodes in sham versus AMI mice with and without NO₂-OA treatment (AMI vehicle: 3.2 ± 2.4 s vs. AMI NO₂-OA: 0.6 ± 0.4 s; n = 8/7). Graphs show Mean ± SEM. Brackets indicate Mean ± SD. *** *P* < 0.001.

NO₂-OA treatment of isolated adult cardiomyocytes under baseline conditions furthermore did not influence the characteristics of Ca²⁺ transients and intracellular Ca²⁺ levels (Supplementary Figure S2).

Given the reduced appearance of spontaneous arrhythmic events upon NO₂-OA treatment after Iso stimulation, we next investigated RyR2-dependent sarcoplasmic calcium leak as a potential pro-arrhythmic molecular mechanism.

Ca²⁺ leak analyses under isoproterenol treatment. Analyses of Ca²⁺ levels in isolated cardiomyocytes showed spontaneous Ca²⁺ peaks after RyR2 unblocking upon Iso stimulation (between the red and black cross in Fig. 4A), whereas almost no arrhythmic events could be observed upon additional NO₂-OA treatment (Fig. 4A, B). Iso treatment resulted in an increased SR-dependent Ca²⁺ leak which was estimated as the difference between the Fura-2 ratio recorded at the end of the 0 Na⁺ / 0 Ca²⁺ Tyrode perfusion (black cross) and at the end of the RyR2 inhibitor tetracaine treatment (red cross) (Fig. 4C). Final caffeine treatment revealed that the SR Ca²⁺ load was not significantly elevated after additional NO₂-OA treatment (Fig. 4D).

Increased SR Ca²⁺ levels have been closely correlated with increased SR Ca²⁺ leak by RyR2-phosphorylation^{29,30}. Of interest, caffeine treatment of short-time paced cardiomyocytes (1 Hz) demonstrated equal SR Ca²⁺ loads in vehicle- and NO₂-OA treated cells. SR Ca²⁺ load was significantly elevated after Iso stimulation, an effect which was slightly, but not significantly, attenuated upon additional NO₂-OA treatment (Supplemental Figure S3).

Ca²⁺ sensitivity. We further investigated the overall influence of NO₂-OA on cytosolic Ca²⁺ levels and arrhythmia development upon increasing Ca²⁺ concentrations (representative Ca²⁺ transients are shown in Fig. 5A). Loading of the cells with Ca²⁺ concentrations ranging from 0.25 to 2 mM enhanced systolic calcium transients (Fig. 5B) as well as diastolic Ca²⁺ levels, the latter of which were not affected by additional NO₂-OA

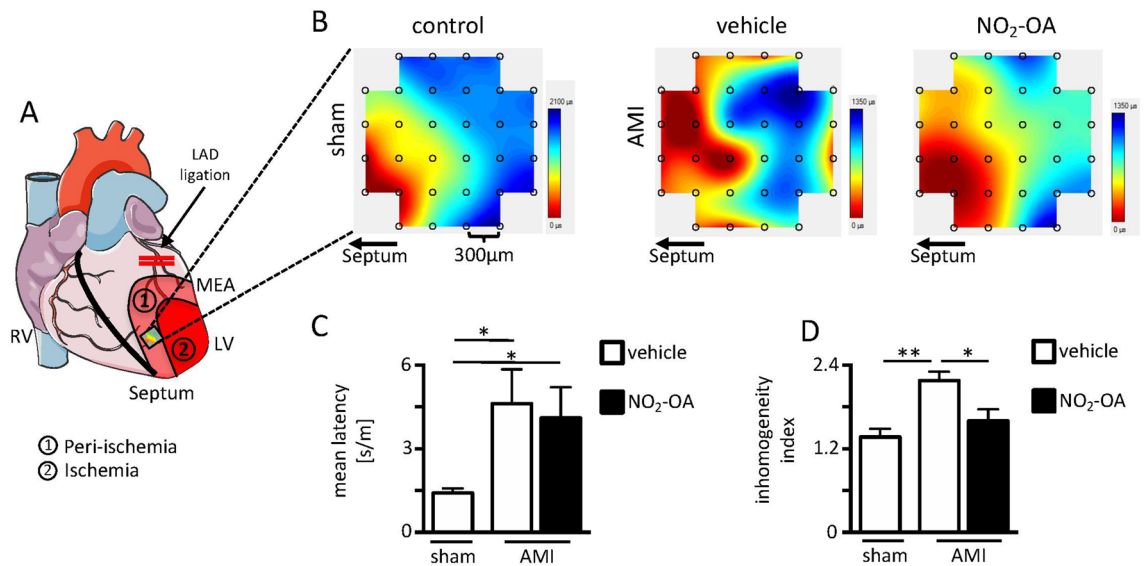


Figure 2. Epicardial mapping analyses within the peri-ischemic region by microelectrode array. (A) Scheme of left ventricular positioning of the multi-electrode array (MEA) indicating ischemic and peri-ischemic regions and cardiac electrical conduction (blue arrows). (B) Representative maps of spontaneous conduction in the peri-ischemic region with vehicle treatment (control) versus treatment with NO₂-OA. Left side of the maps indicate electrodes oriented nearest to myocardial septum as shown in A. (C) Mean inter-electrode latency of electrical conduction (sham vehicle: 1.4 ± 0.5 s/m vs. AMI vehicle: 4.6 ± 3.3 s/m vs. AMI NO₂-OA: 4.1 ± 2.9 s/m; n = 8/7/7) and (D) inhomogeneity index in sham animals versus 20 min of ischemia with and without NO₂-OA treatment (sham vehicle: 1.4 ± 0.3 vs. AMI vehicle: 2.2 ± 0.3 vs. AMI NO₂-OA: 1.6 ± 0.4; n = 8/7/7). Interelectrode distance = 300 μm. Graphs show Mean ± SEM. Brackets indicate Mean ± SD. * $P < 0.05$; ** $P < 0.01$. Figures were produced using Servier Medical Art (<https://www.servier.com/>).

treatment (Fig. 5C). Of importance, NO₂-OA treatment completely inhibited Iso induced arrhythmic Ca²⁺ release (Fig. 5D).

Catecholamine-induced CaMKII activity and RyR2 phosphorylation. Given its importance in RyR2 activity and dysfunction, we next investigated the effect of NO₂-OA treatment on CaMKII activity by performing a substrate binding assay using GST-HDAC4 419-670, which contains a CaMKII activity-dependent binding site³¹. CaMKII activity of Iso stimulated isolated cardiomyocytes was significantly reduced after NO₂-OA treatment (Fig. 6A). In accordance, NO₂-OA markedly diminished the Iso induced increase of pro-arrhythmic RyR2 phosphorylation on Ser2814³² as revealed by immunoblotting (Fig. 6B). CaMKII-mediated Thr17-phosphorylation of PLN, which enhances sarcoplasmic reticulum (SR) Ca²⁺-ATPase (SERCA2a) activity³³, was increased upon Iso treatment and not further affected by NO₂-OA treatment (Fig. 6C).

Discussion

Herein, we show that the electrophilic fatty acid nitroalkene NO₂-OA prevents induction of VT after AMI in vivo by attenuating CaMKII dependent RyR2 leak. These results are of significant clinical relevance since sudden cardiac death related to AMI is most frequently attributed to the occurrence of sustained VT or ventricular fibrillation (VF)³⁴. Although the absolute rates of VT and VF have declined during the era of percutaneous coronary intervention, patients suffering from VT or VF prior to revascularization still have a significantly impaired outcome and are at a higher risk for stent thrombosis. These data may underestimate the true incidence, since prehospital SCD before fibrinolysis or any other interventions were not included in this analysis³⁵. In the present study, we modeled a clinical scenario of myocardial ischemia by LAD ligation and demonstrated that intraperitoneal injection of NO₂-OA 20 min before the ischemic episode sustainably reduced ventricular arrhythmic events specifically in the acute phase after AMI.

The prospect of using NO₂-OA as a therapeutic option for the treatment of acute VT after AMI is underlined by further beneficial effects of this fatty acid nitroalkenes in various cardiovascular diseases. As we and others have demonstrated, the application of NO₂-OA preserves left ventricular ejection fraction and reduces infarct size in a mouse model of AMI^{19,36}. Moreover, NO₂-OA also protects from angiotensin II induced atrial fibrillation¹².

Mechanistically, the occurrence of ventricular arrhythmic events during the acute phase of AMI is attributed to development of proarrhythmic substrates with subsequent formation of reentry circuits³. The concomitantly enhanced sympathetic tone leads to cellular Ca²⁺ overload, resulting in a disturbed Ca²⁺ homeostasis, accompanied by diastolic Ca²⁺ leak further increasing the vulnerability for VT³⁷. On a cellular level, alterations in Ca²⁺ transients have been linked to the emergence of alternans and afterdepolarizations which may trigger VTs⁴, as well as to reduced sodium channel availability resulting in ventricular conduction slowing. This increases the wavelength of reentry circuits thereby increasing the vulnerability to VTs³⁸⁻⁴⁰.

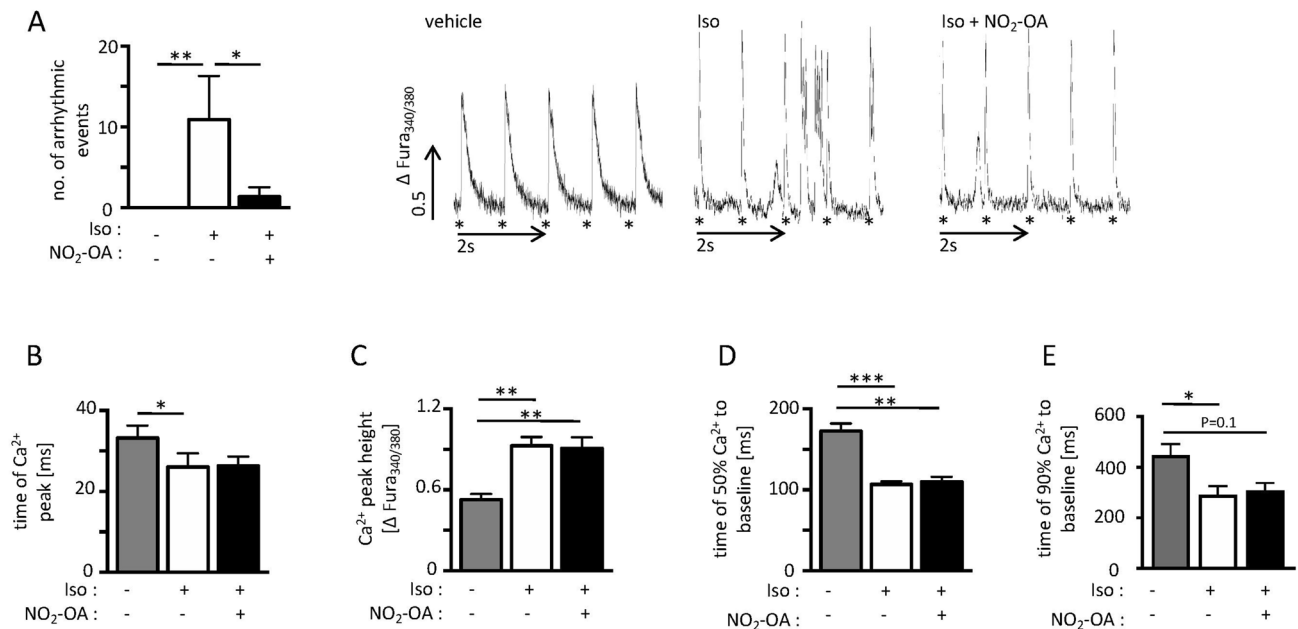


Figure 3. Rhythm analyses and Ca²⁺ transient measurements of isolated adult cardiomyocytes under beta-adrenergic stimulation. **(A)** Number of arrhythmic events and representative recordings of calcium transients of isolated adult cardiomyocytes with and without Iso and Iso + NO₂-OA treatment (vehicle: 0.0 ± 0.0 vs. Iso: 10.9 ± 18.6 vs. Iso + NO₂-OA: 1.4 ± 3.9; n(cells out of 3 animals) = 9/12/11). Asterisks indicate time point of external stimulation. **(B)** Time to maximum Ca²⁺ peak as indicator for Ca²⁺ influx velocity (vehicle: 33.2 ± 9.3 ms vs. Iso: 26.1 ± 13.1 ms vs. Iso + NO₂-OA: 26.3 ± 8.4 ms; n(cells out of 3 animals) = 9/15/13). **(C)** Relative Ca²⁺ peak height as indicator for the maximal amount of Ca²⁺ in control- versus Iso- and Iso + NO₂-OA treated cells (vehicle: 0.53 ± 0.12 vs. Iso: 0.93 ± 0.25 vs. Iso + NO₂-OA: 0.91 ± 0.29 ms; n(cells out of 3 animals) = 9/15/13). **(D)** Time to 50% Ca²⁺ decay (vehicle: 173.7 ± 35.9 ms vs. Iso: 106.4 ± 22.8 ms vs. Iso + NO₂-OA: 89.9 ± 17.8 ms; n(cells out of 3 animals) = 9/14/13) and € 90% Ca²⁺ decay as indicators for cytosolic Ca²⁺ clearance (vehicle: 448.0 ± 12.5 ms vs. Iso: 291.1 ± 12.8 ms vs. Iso + NO₂-OA: 308.0 ± 10.3 ms; n (cells out of 3 animals) = 8/14/12). Graphs show Mean ± SEM. Brackets indicate Mean ± SD. **P* < 0.05; ***P* < 0.01; ****P* < 0.001.

To investigate the effects of NO₂-OA on cellular Ca²⁺ transients and sarcoplasmic Ca²⁺ load, both important in arrhythmia development in AMI, we performed analyses of electrically stimulated isolated cardiomyocytes. We did not detect major changes in both Ca²⁺ transient characteristics and in SR Ca²⁺ load upon NO₂-OA treatment.

We quantified PLN phosphorylation, a protein regulating cytosolic Ca²⁺ clearance into the SR by SERCA2a⁵, at its CaMKII specific phosphorylation site Thr17 under Iso stimulation. Iso increased PLN phosphorylation but no further change was detectable upon treatment with NO₂-OA. This indicates that NO₂-OA does not influence cytosolic Ca²⁺ clearance by CaMKII mediated phosphorylation of PLN on this specific site, although we could not fully exclude potential other target sites or phosphorylation mechanisms being modified by NO₂-OA.

To further examine the underlying molecular effects of NO₂-OA-mediated VT prevention in detail, we measured RyR2-dependent Ca²⁺ leak from the SR in isolated adult cardiomyocytes treated with Iso. We observed an increased number of arrhythmic events (e.g. EADs and DADs) upon Iso treatment that was markedly reduced by NO₂-OA. Therefore, we hypothesized that NO₂-OA beneficially influences CaMKII-dependent modulation of Ca²⁺-homeostasis. Indeed, CaMKII activity and subsequent RyR2 phosphorylation on the critical serine residue (Ser2814), which has been linked to CaMKII-mediated Ca²⁺ leak in cardiomyopathy and catecholamine treatment⁴¹, was significantly attenuated by NO₂-OA in Iso-stressed cardiomyocytes (Fig. 6B). These results are in accordance with recent data demonstrating that increased RyR2 phosphorylation and thereby altered Ca²⁺ sensitivity may lead to local Ca²⁺ waves, subsequently depolarizing the membrane potential and forming DADs. These local events furthermore trigger Ca²⁺ waves in adjacent cells and create propagating arrhythmic events⁴².

Speculating on underlying biochemical mechanisms, it is noted that CaMKII activity and subsequent RyR2 phosphorylation is regulated by S-nitrosylation of specific cysteines (e.g. Cys273/ Cys290)⁴³. Previous work shows that NO₂-OA could act as a NO-donor for S-nitrosylation via a modified Nef reaction. This minor and controversial reaction, as opposed to the signaling responses induced by the post-translational alkylation of protein thiols, occurs in very low yields and only yields NO in aqueous buffered solutions when no protein is present⁴⁴. Thus, it is anticipated that under pathological conditions, NO₂-OA acts via a reversible nitroalkylation of functionally-significant cysteines^{11,19}. The further investigation of critical protein targets in this model of cardioprotection will be the subject of further studies.

As this study was performed in a small animal model, a number of limitations may apply when trying to translate the present findings to human pathology. The mechanisms underlying VT in the setting of AMI are the result of multiple alterations, e.g. loss of viable myocardium with loss of cell-to-cell contact, changes in cell

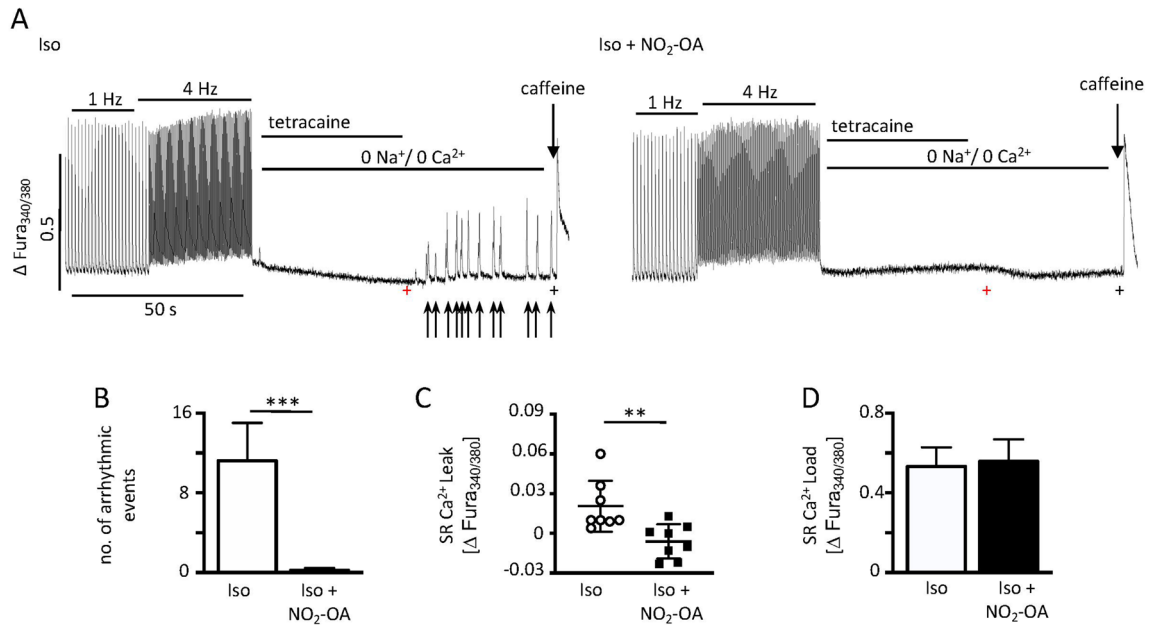


Figure 4. Iso dependent Ca²⁺ leak analyses in isolated adult cardiomyocytes. **(A)** Representative Ca²⁺ transient recordings of isolated adult isoproterenol (Iso)- and Iso + NO₂-OA treated cardiomyocytes upon field stimulation (1 Hz and 4 Hz) followed by assessment of Ca²⁺ leak under non-stimulated conditions after removal of the RyR2 inhibitor tetracaine. Arrows indicate spontaneous arrhythmic events (red and black crosses visualize time points of Fura-2 ratios used for Ca²⁺ leak calculation). **(B)** Total number of arrhythmic events after removal of tetracaine (between red and black crosses) of Iso or Iso + NO₂-OA subjected isolated cardiomyocytes (Iso: 11.2 ± 11.42 vs. Iso + NO₂-OA: 0.2 ± 0.67 ; $n = 8/8$). **(C)** Sarcoplasmic (SR) Ca²⁺ leak quantified as Δ Fura-2 ratio (Iso: 0.021 ± 0.019 Δ Fura-2 ratio vs. Iso + NO₂-OA: -0.006 ± 0.013 Δ Fura-2 ratio). **(D)** Total SR Ca²⁺ load in Iso versus Iso + NO₂-OA treated cardiomyocytes (Iso: 0.53 ± 0.29 vs. Iso + NO₂-OA: 0.56 ± 0.33). **(B–D)** n (cells out of 3 animals) = 8/8. Graphs show Mean \pm SEM. Brackets indicate Mean \pm SD. ** $P < 0.01$; *** $P < 0.001$.

membrane potential, ion composition, and other factors predisposing for sudden cardiac death which are only partly mirrored by our experimental setting³.

Excessive catecholamine stimulation may be just one of multiple pathways leading to VT development during AMI modulated by NO₂-OA. However, if other mechanisms, e.g., those responsive to acidosis and cell hypoxia, are altered by NO₂-OA remains to be investigated.

In summary, we show for the first time that, by inhibiting CaMKII, NO₂-OA modulates a critical pathway of electrical remodeling following AMI and thus has potential as a pre-emptive anti-arrhythmic strategy for patients at risk for developing AMI.

Conclusions and perspectives

Our current data reveal that NO₂-OA rapidly stabilizes myocellular Ca²⁺ homeostasis by inhibition of CaMKII activity in the setting of AMI (Fig. 7). Crucially, herein we show for the first time that, by modulation of this pathway, NO₂-OA markedly suppresses the susceptibility to ventricular arrhythmias.

There are limited treatment options for prevention of acute arrhythmic tachycardias within the first 72 h after AMI, especially considering the amount of time to reach therapeutic levels for available drugs⁴⁵. In this regard, the long-term dietary supplementation of NO₂-OA or its precursors, might be a therapeutic option to protect AMI patients against subsequent VT / SCD.

Materials and methods

An extended description of the methods can be found within the Supplemental Material.

Animal studies. Male, 8- to 12-week old FVB/N mice (Charles River) were used for all animal studies. All animal studies were approved by the local Animal Care and Use Committees (Ministry for Environment, Agriculture, Conservation and Consumer Protection of the State of North Rhine-Westphalia: State Agency for Nature, Environment and Consumer Protection (LANUV), NRW, Germany) and follow ARRIVE (Animal Research: Reporting of In Vivo Experiments) guidelines.

Left anterior descending artery (LAD) ligation. LAD ligation to induce myocardial ischemia was performed as described by Mollenhauer et al.²⁶.

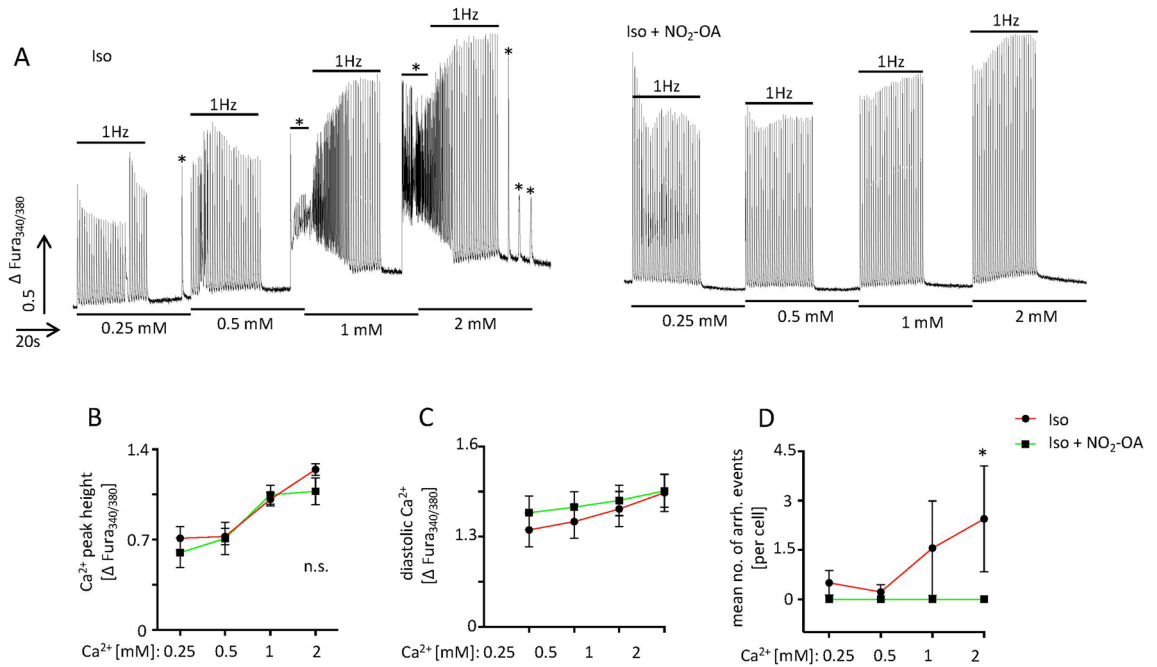


Figure 5. Ca²⁺ sensitivity analyses in isolated adult cardiomyocytes. **(A)** Representative Ca²⁺ transient recordings of isolated adult isoproterenol (Iso)- and Iso + NO₂-OA treated cardiomyocytes upon increasing extracellular Ca²⁺ concentrations (0.25 mM–2 mM) stimulated at 1 Hz for 30 s following a non-stimulated period of 20 s in which arrhythmic Ca²⁺ events were recorded (asterisks). **(B)** Relative Ca²⁺ transient peak height in control- versus Iso- and Iso + NO₂-OA treated cells upon different Ca²⁺ concentrations (Iso vs. Iso + NO₂-OA [ΔFura-2]); 0.25 mM Ca²⁺: 0.71 ± 0.28 vs. 0.6 ± 0.23; 0.5 mM Ca²⁺: 0.73 ± 0.19 vs. 0.71 ± 0.28; 1 mM Ca²⁺: 1.01 ± 0.16 vs. 1.05 ± 0.16; 2 mM Ca²⁺: 1.24 ± 0.14 vs. 1.08 ± 0.23). **(C)** Relative diastolic Ca²⁺ levels measured between the 1 Hz pacing periods (Iso vs. Iso + NO₂-OA [ΔFura-2]); 0.25 mM Ca²⁺: 1.32 ± 0.16 vs. 1.38 ± 0.13; 0.5 mM Ca²⁺: 1.35 ± 0.16 vs. 1.40 ± 0.11; 1 mM Ca²⁺: 1.39 ± 0.16 vs. 1.42 ± 0.11; 2 mM Ca²⁺: 1.45 ± 0.18 vs. 1.45 ± 0.12). **(D)** Mean number of arrhythmic Ca²⁺ release events within the non-stimulated time period (asterisks, Iso vs. Iso + NO₂-OA [mean number]); 0.25 mM Ca²⁺: 0.5 ± 1.07 vs. 0.0 ± 0.0; 0.5 mM Ca²⁺: 0.22 ± 0.67 vs. 0.0 ± 0.0; 1 mM Ca²⁺: 1.56 ± 4.3 vs. 0.0 ± 0.0; 2 mM Ca²⁺: 2.44 ± 4.82 vs. 0.0 ± 0.0). **(B–D)** n(cells out of 3 animals) = 9/5 for each concentration. Graphs show Mean ± SEM. Brackets indicate Mean ± SD. * *P* < 0.05.

Right ventricular stimulation. A detailed stimulation protocol can be found within the Supplemental Material. In short, right ventricular stimulation was performed 20 min after induction of myocardial ischemia, while the mouse was kept under anesthesia, according to a standardized protocol that initially included a programmed ventricular stimulation with a fixed S1S1 interval to whose last S1-impulse a short-coupled additional stimulus was applied. After 10 s of recovery, automated burst stimulation was performed according to the protocol. VT were defined as a series of repetitive ventricular ectopic beats lasting for > 200 ms²⁶.

In vivo electrophysiological mapping. In brief, directly after electrophysiological investigation the heart was exposed by thoracotomy. A 32-electrode microelectrode array (MEA, Multichannel Systems, Reutlingen, Germany) was positioned on the epicardial surface of the left ventricle apico-septally of the peri-ischemic region as described previously²⁶. Field potentials were recorded using a 128-channel, computer-assisted recording system (Multichannel Systems). Data was evaluated according to Lammers et al.⁴⁶. In short, inter-electrode conduction latencies (reciprocal conduction velocity) were calculated for all neighboring electrodes. Of each neighboring quadruplet of electrodes, the largest latency was taken and plotted as a phase map. From this phase map the mean latency of conduction was calculated. The variation coefficient of the phase map was calculated (Percentile (P): P₅₋₉₅/P₅₀) to receive the index of inhomogeneity as velocity independent factor of conduction inhomogeneity. Phase maps were calculated using custom-programmed software (Excel).

Administration of nitro-oleic acid. Nitro-oleic acid (9- and 10-nitro-octadec-9-cis-enoic acid; NO₂-OA), administered at 20 nmol/g body weight, was solvated in polyethylene-glycol/ethanol (85:15, vol/vol), or 100 ml of vehicle (polyethylene-glycol/ ethanol, 85:15). These preparations were injected i.p. 20 min prior to LAD ligation. NO₂-OA was synthesized as previously described⁴⁷.

Isolation of adult ventricular cardiomyocytes. Ventricular myocytes were obtained from 8 to 12 week old male wild-type mice (FVB/N) as described previously²⁸.

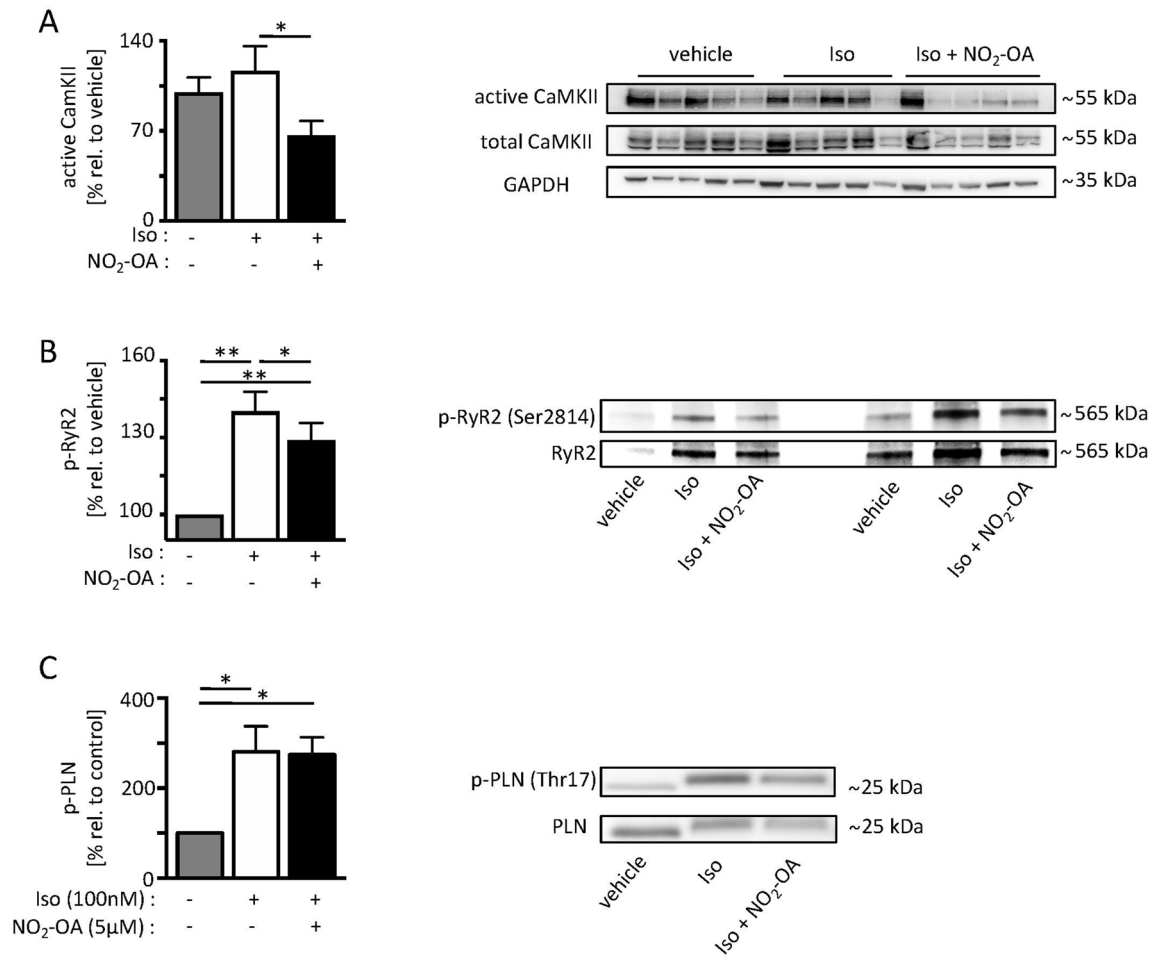


Figure 6. CaMKII activity and RyR2 phosphorylation upon beta-adrenergic stimulation in isolated adult cardiomyocytes. **(A)** Immunoblot analyses after GST pulldown showing active (GST-HDAC4 419-670-bound) CaMKII in relation to total CaMKII (vehicle: 100% ± 36.1 vs. Iso: 116.5% ± 57.9 vs. Iso + NO₂-OA: 66% ± 34.4). **(B)** Critical RyR2 phosphorylation under Iso stimulation and simultaneous NO₂-OA treatment as indicated by immunoblotting (vehicle: 100% vs. Iso: 140% ± 22.9 vs. NO₂-OA: 129% ± 19.8). **(C)** Phosphorylation of phospholamban (Thr17-p-PLN) in vehicle- vs. Iso- vs. Iso + NO₂-OA treated cardiomyocytes (vehicle: 100% vs. Iso: 107.2% ± 0.1 vs. NO₂-OA: 107.0% ± 2.9). n (cells out of 3 animals) = 9/9/9. Graphs show Mean ± SEM. Brackets indicate Mean ± SD. * $P < 0.05$; ** $P < 0.01$; *** $P < 0.001$. The cropped blots are presented, and their full-length blots are included in the Supplemental Figures S4–S6.

Assessment of Ca²⁺ transients. All experiments were performed at 37 °C within 6 h after cell isolation, as described previously using ratiometric Ca²⁺ imaging with Fura-2 dye (IonOptix)²⁸.

For Ca²⁺ transient analyses the cells were incubated with either 0.1% EtOH as control, 10 μM Iso in 0.1% EtOH or 10 μM Iso and 5 μM NO₂-OA in 0.1% EtOH for 10 min. Calcium transients were recorded under electrically stimulated biphasic field pulses (20 V, 4 ms) at a frequency of 1 Hz for 1 min.

SR Ca²⁺ leak and load were measured according to a modified protocol^{28,48}. Fura-2 loaded ventricular cardiomyocytes were incubated with 10 μM Iso for 7 min and stimulated for 3 min at 1 Hz, 20 V, 4 ms until cellular Ca²⁺ transients reached a steady state followed by a burst stimulation with 4 Hz for 30 s. Directly after the last pulse the pacing was stopped and the normal Tyrode solution was substituted by a 0 Na⁺ / 0 Ca²⁺ Tyrode supplemented with 10 mmol/l EGTA and 1 mmol/l of the RyR2 inhibitor tetracaine in which Na⁺ was replaced by Li⁺. This condition allowed measuring intracellular Ca²⁺ levels in a closed system without trans-sarcolemmal Ca²⁺ fluxes and prevents SR Ca²⁺ leak into the cytoplasm. After 40 s recording time the solution was switched back to 0 Na⁺ / 0 Ca²⁺ Tyrode without tetracaine for another 40 s to unblock the ryanodine receptors and allow potential Ca²⁺ leak. SR Ca²⁺ leak was estimated as the difference between the Fura-2 ratio recorded at the end of the 0 Na⁺ / 0 Ca²⁺ Tyrode perfusion with and without tetracaine. At the end of the protocol, 10 mM caffeine was applied to evaluate the total SR Ca²⁺ content.

Ca²⁺ sensitivity: Fura-2 loaded ventricular cardiomyocytes were incubated with Tyrode solution containing 0.25 mM, 0.5 mM, 1 mM or 2 mM of Ca²⁺ together with either 10 μM Iso in 0.1% EtOH or 10 μM Iso and 5 μM NO₂-OA in 0.1% EtOH. For each calcium concentration cells were paced at 1 Hz for 30 s following a 20 s non-pacing period in which pro-arrhythmic calcium release events was counted. Ca²⁺ transient height was determined within the last paced Ca²⁺ transient before the non-paced period.

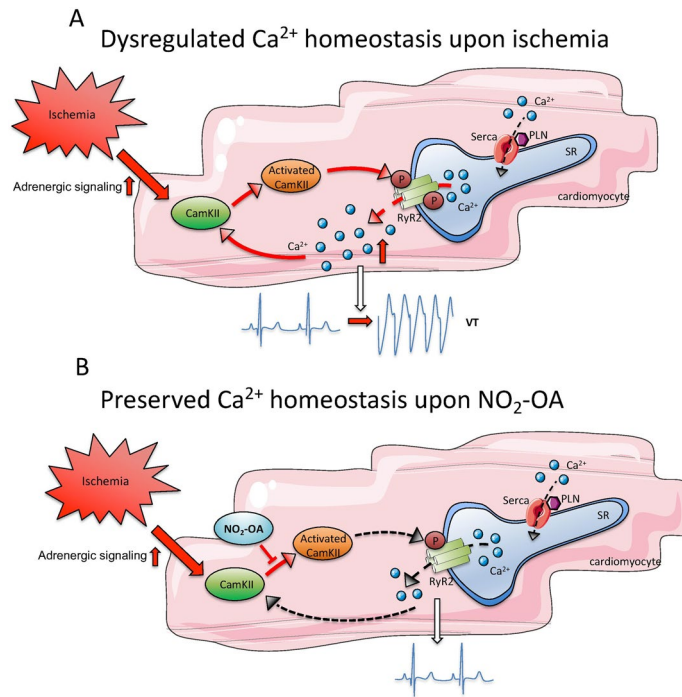


Figure 7. NO₂-OA prevents acute ischemia induced ventricular tachycardias. **(A)** Increased adrenergic signaling leads to the activation of CaMKII with subsequently dysregulated RyR2-function and impaired Ca²⁺ homeostasis due to a diastolic Ca²⁺ leak. **(B)** Treatment with NO₂-OA restores Ca²⁺ homeostasis and prevents ventricular tachycardia (VT) development. Figures were produced using Servier Medical Art (<https://www.servier.com/>).

Ca²⁺ transient characteristics were calculated by the IonWizard (IonOptix) software.

Immunoblotting. Protein extraction and immunoblotting were performed as previously described²⁶. Briefly, membranes were incubated with the following antibodies overnight at 4 °C: anti-GAPDH (1:1000; Santa Cruz), anti-P-PLN-Thr17, anti-PLN, anti-P-RyR2-Ser2814 (1:5000; Badrilla), anti-RyR2 (1:2000; Sigma-Aldrich). Full blots are shown in the Supplemental Material section.

CaMKII activity assay. CaMKII activity was assessed by detecting the amount of endogenous CaMKII that binds to GST-HDAC4 amino acids 419 to 670 (containing the CaMKII activity-dependent binding domain) as described previously³¹. Bound active CaMKII, CaMKII input, and GST-HDAC4 419-670 input were resolved by SDS-PAGE and detected by immunoblot using HDAC4 (1:1000; Santa Cruz) and CaMKII antibodies (1:1000; BD Bioscience). Protein loading was normalized to GAPDH (1:10000; Sigma-Aldrich).

Statistical analysis. Results are expressed as mean ± standard error of the mean. Gaussian normality was tested via Shapiro–Wilk normality test. Unpaired Student’s t-test or one-way ANOVA were used for gaussian distributed data, whereas non-gaussian distributed data were analyzed using Kruskal Wallis test, each followed by appropriate post-hoc test. Results of Fig. 5B, C are normalized against their respective control within the same animal. An alpha level of $P < 0.05$ was considered statistically significant. All statistical calculations were carried out using GraphPad Prism 8.2.1 (GraphPad). * $P < 0.05$, ** $P < 0.01$, *** $P < 0.001$.

Received: 12 December 2019; Accepted: 22 July 2020

Published online: 18 September 2020

References

- McManus, D. D. *et al.* Recent trends in the incidence, treatment, and outcomes of patients with STEMI and NSTEMI. *Am. J. Med.* **124**, 40–47 (2011).
- Piccini, J. P., Berger, J. S. & Brown, D. L. Early sustained ventricular arrhythmias complicating acute myocardial infarction. *Am. J. Med.* **121**, 797–804 (2008).
- Di Diego, J. M. & Antzelevitch, C. Ischemic ventricular arrhythmias: experimental models and their clinical relevance. *Heart. Rhythm* **8**, 1963–1968 (2011).
- Landstrom, A. P., Dobrev, D. & Wehrens, X. H. T. Calcium signaling and cardiac arrhythmias. *Circ. Res.* **120**, 1969–1993 (2017).

5. Grimm, M. & Brown, J. H. Beta-adrenergic receptor signaling in the heart: role of CaMKII. *J. Mol. Cell. Cardiol.* **48**, 322–330 (2010).
6. Swaminathan, P. D., Purohit, A., Hund, T. J. & Anderson, M. E. Calmodulin-dependent protein kinase II: linking heart failure and arrhythmias. *Circ. Res.* **110**, 1661–1677 (2012).
7. Carmeliet, E. Cardiac ionic currents and acute ischemia: from channels to arrhythmias. *Physiol. Rev.* **79**, 917–1017 (1999).
8. Bhatt, D. L. *et al.* Cardiovascular risk reduction with icosapent ethyl for hypertriglyceridemia. *N. Engl. J. Med.* **380**, 11–22 (2019).
9. Rubbo, H. *et al.* Nitric oxide regulation of superoxide and peroxynitrite-dependent lipid peroxidation: formation of novel nitrogen-containing oxidized lipid derivatives. *J. Biol. Chem.* **269**, 26066–26075 (1994).
10. Khoo, N. K. H. *et al.* Activation of vascular endothelial nitric oxide synthase and heme oxygenase-1 expression by electrophilic nitro-fatty acids. *Free Radic. Biol. Med.* **48**, 230–239 (2010).
11. Baker, L. M. S. *et al.* Nitro-fatty acid reaction with glutathione and cysteine: kinetic analysis of thiol alkylation by a Michael addition reaction. *J. Biol. Chem.* **282**, 31085–31093 (2007).
12. Rudolph, T. K. *et al.* Nitrated fatty acids suppress angiotensin II-mediated fibrotic remodelling and atrial fibrillation. *Cardiovasc. Res.* **109**, 174–184 (2016).
13. Rudolph, T. K. *et al.* Nitro-fatty acids reduce atherosclerosis in apolipoprotein E-deficient mice. *Arterioscler. Thromb. Vasc. Biol.* **30**, 938–945 (2010).
14. Bonacci, G. *et al.* Electrophilic fatty acids regulate matrix metalloproteinase activity and expression. *J. Biol. Chem.* **286**, 16074–16081 (2011).
15. Khoo, N. K. H. & Freeman, B. A. Electrophilic nitro-fatty acids: anti-inflammatory mediators in the vascular compartment. *Curr. Opin. Pharmacol.* **10**, 179–184 (2010).
16. Rudolph, V. *et al.* Nitro-fatty acid metabolome: saturation, desaturation, β -oxidation, and protein adduction. *J. Biol. Chem.* **284**, 1461–1473 (2009).
17. Mollenhauer, M., Mehrkens, D. & Rudolph, V. Nitrated fatty acids in cardiovascular diseases. *Nitric Oxide* **78**, 146–153 (2018).
18. Nadtochiy, S. M., Baker, P. R. S., Freeman, B. A. & Brookes, P. S. Mitochondrial nitroalkene formation and mild uncoupling in ischaemic preconditioning: implications for cardioprotection. *Cardiovasc. Res.* **82**, 333–340 (2009).
19. Rudolph, V. *et al.* Endogenous generation and protective effects of nitro-fatty acids in a murine model of focal cardiac ischaemia and reperfusion. *Cardiovasc. Res.* **85**, 155–166 (2010).
20. Arbeeny, C. M. *et al.* CXA-10, a nitrated fatty acid, is renoprotective in deoxycorticosterone acetate-salt nephropathy. *J. Pharmacol. Exp. Ther.* **369**, 503–510 (2019).
21. Open-Label Safety, Tolerability, PK Study of IV CXA-10 Emulsion in Subjects in Chronic Kidney Injury - Full Text View - ClinicalTrials.gov. Available at: <https://clinicaltrials.gov/ct2/show/study/NCT02248051>. Accessed: 18 Sept 2019
22. FIRSTx - A Study of Oral CXA-10 in Primary Focal Segmental Glomerulosclerosis (FSGS) - Full Text View - ClinicalTrials.gov. Available at: <https://clinicaltrials.gov/ct2/show/NCT03422510?term=nitro+fatty+acid&rank=3>. Accessed 18 Sept 2019
23. CXA-10 study in subjects with pulmonary arterial hypertension —full text view - clinicaltrials.gov. Available at: <https://clinicaltrials.gov/ct2/show/NCT04053543?term=CXA-10&rank=1>. Accessed 18 Sept 2019
24. Tsikas, D., Zoerner, A. A., Mitschke, A. & Gutzki, F.-M. Nitro-fatty acids occur in human plasma in the picomolar range: a targeted nitro-lipidomics GC-MS/MS study. *Lipids* **44**, 855–865 (2009).
25. Bonacci, G. *et al.* Conjugated linoleic acid is a preferential substrate for fatty acid nitration. *J. Biol. Chem.* **287**, 44071–44082 (2012).
26. Mollenhauer, M. *et al.* Myeloperoxidase mediates postischemic arrhythmogenic ventricular remodeling. *Circ. Res.* CIRCRESAHA.117.310870 (2017). <https://doi.org/10.1161/CIRCRESAHA.117.310870>
27. Antzelevitch, C. & Burashnikov, A. Overview of basic mechanisms of cardiac arrhythmia. *Card. Electrophysiol. Clin.* **3**, 23–45 (2011).
28. Vettel, C. *et al.* Phosphodiesterase 2 protects against catecholamine-induced arrhythmia and preserves contractile function after myocardial infarction. *Circ. Res.* **120**, 120–132 (2017).
29. Blayney, L. M. & Lai, F. A. Ryanodine receptor-mediated arrhythmias and sudden cardiac death. *Pharmacol. Ther.* **123**, 151–177 (2009).
30. Lyon, A. R. *et al.* SERCA2a gene transfer decreases sarcoplasmic reticulum calcium leak and reduces ventricular arrhythmias in a model of chronic heart failure. *Circ. Arrhythmia Electrophysiol.* **4**, 362–372 (2011).
31. Dewenter, M. *et al.* Calcium/calmodulin-dependent protein Kinase II activity persists during chronic β -adrenoceptor blockade in experimental and human heart failure. *Circ. Hear. Fail.* **10**, (2017).
32. Voigt, N. *et al.* Enhanced sarcoplasmic reticulum Ca²⁺ leak and increased Na⁺-Ca²⁺ exchanger function underlie delayed afterdepolarizations in patients with chronic atrial fibrillation. *Circulation* **125**, 2059–2070 (2012).
33. Mattiazzi, A., Mundinawellenmann, C., Guoxiang, C., Vittoni, L. & Kranias, E. Role of phospholamban phosphorylation on Thr17 in cardiac physiological and pathological conditions. *Cardiovasc. Res.* **68**, 366–375 (2005).
34. Kosmidou, I. *et al.* Early ventricular tachycardia or fibrillation in patients With ST elevation myocardial infarction undergoing primary percutaneous coronary intervention and impact on mortality and stent thrombosis (from the harmonizing outcomes with revascularization and stents in acute myocardial infarction trial). *Am. J. Cardiol.* **120**, 1755–1760 (2017).
35. Thomas, D. E., Jex, N. & Thornley, A. R. Ventricular arrhythmias in acute coronary syndromes-mechanisms and management. *Contin. Cardiol. Educ.* **3**, 22–29 (2017).
36. Qipshidze-Kelm, N., Piell, K. M., Solinger, J. C. & Cole, M. P. Co-treatment with conjugated linoleic acid and nitrite protects against myocardial infarction. *Redox Biol.* **2**, 1–7 (2014).
37. Kirchhof, P. *et al.* Ventricular arrhythmias, increased cardiac calmodulin kinase II expression, and altered repolarization kinetics in ANP receptor deficient mice. *J. Mol. Cell. Cardiol.* **36**, 691–700 (2004).
38. Salvage, S. C. *et al.* Flecainide exerts paradoxical effects on sodium currents and atrial arrhythmia in murine RyR2-P2328S hearts. *Acta Physiol.* **214**, 361–375 (2015).
39. Denham, N. C. *et al.* Calcium in the pathophysiology of atrial fibrillation and heart failure. *Front. Physiol.* **9**, (2018).
40. Kanaporis, G. & Blatter, L. A. The mechanisms of calcium cycling and action potential dynamics in cardiac alternans. *Circ. Res.* **116**, 846–856 (2015).
41. Grimm, M. *et al.* CaMKII δ mediates β -adrenergic effects on RyR2 phosphorylation and SR Ca(2+) leak and the pathophysiological response to chronic β -adrenergic stimulation. *J. Mol. Cell. Cardiol.* **85**, 282–291 (2015).
42. Boyden, P. A. & Smith, G. L. Ca²⁺ leak—what is it? Why should we care? Can it be managed?. *Hear. Rhythm* **15**, 607–614 (2018).
43. Erickson, J. R. *et al.* S-Nitrosylation induces both autonomous activation and inhibition of calcium/calmodulin-dependent protein kinase II δ . *J. Biol. Chem.* **290**, 25646 (2015).
44. Su, Y.-H., Wu, S.-S. & Hu, C.-H. Release of nitric oxide from nitrated fatty acids: Insights from computational chemistry. *J. Chin. Chem. Soc.* **66**, 41–48 (2019).
45. Bhar-Amato, J., Davies, W. & Agarwal, S. Ventricular arrhythmia after acute myocardial infarction: 'the perfect storm'. *Arrhythmia Electrophysiol. Rev.* **6**, 134–139 (2017).
46. Lammers, W. J., Schalij, M. J., Kirchhof, C. J. & Allessie, M. A. Quantification of spatial inhomogeneity in conduction and initiation of reentrant atrial arrhythmias. *Am. J. Physiol.* **259**, H1254–H1263 (1990).

47. Baker, P. R. S. *et al.* Fatty acid transduction of nitric oxide signaling: multiple nitrated unsaturated fatty acid derivatives exist in human blood and urine and serve as endogenous peroxisome proliferator-activated receptor ligands. *J. Biol. Chem.* **280**, 42464–42475 (2005).
48. Shannon, T. R., Ginsburg, K. S. & Bers, D. M. Quantitative assessment of the SR Ca²⁺ leak-load relationship. *Circ. Res.* **91**, 594–600 (2002).

Acknowledgements

We thank Romy Kempe for expert technical assistance. We thank Servier Medical Art for providing medical images (<https://www.servier.com>).

Author contributions

The author contributions are as follows: M.M., D.M., S.B., V.R. designed the project, performed experiments and statistical analysis and prepared the manuscript. D.M., A.K., M.L., L.R., K.F., S.Br., S.G., S.S., F. S. N., S.L., G.P., A.C.G., B.G., A.P.S., M.D., X.L., M.W. and M.A., performed experiments and provide suggestions on the project. L.C., B.A.F., A.E.A. provide substantial suggestions on the project and critically revised the manuscript and B.A.F. provided the nitro-oleic acid. S.B., V.R. supervised the project. M.M. supervised the project and wrote the manuscript. All authors have reviewed the manuscript and approved the submission.

Funding

This work was supported by the Deutsche Forschungsgemeinschaft (RU 1678/3-1, RU 1678/3-3 to Volker Rudolph, GRK 2407 (360043781) to Volker Rudolph and Dennis Mehrkens, EL 270/7-1 to Ali El-Armouche, WA 2586/4-1 to Michael Wagner, SFB TRR259 (397484323) Project—A04 for Stephan Baldus and Project—B05 for Matti Adam) and the Center for Molecular Medicine Cologne funding (Baldus B-02). Open access funding provided by Projekt DEAL.

Competing interests

B.A.F. has financial interest in Complexa Inc. and Creegh Pharmaceuticals. All other authors declare that they have no conflicts of interest with the contents of this article.

Additional information

Supplementary information is available for this paper at <https://doi.org/10.1038/s41598-020-71870-6>.

Correspondence and requests for materials should be addressed to M.M.

Reprints and permissions information is available at www.nature.com/reprints.

Publisher's note Springer Nature remains neutral with regard to jurisdictional claims in published maps and institutional affiliations.



Open Access This article is licensed under a Creative Commons Attribution 4.0 International License, which permits use, sharing, adaptation, distribution and reproduction in any medium or format, as long as you give appropriate credit to the original author(s) and the source, provide a link to the Creative Commons licence, and indicate if changes were made. The images or other third party material in this article are included in the article's Creative Commons licence, unless indicated otherwise in a credit line to the material. If material is not included in the article's Creative Commons licence and your intended use is not permitted by statutory regulation or exceeds the permitted use, you will need to obtain permission directly from the copyright holder. To view a copy of this licence, visit <http://creativecommons.org/licenses/by/4.0/>.

© The Author(s) 2020